WOOD RESEARCH
54 (2): 2009
49-62

INVESTIGATION OF THE MECHANISM OF FAILURE BEHAVIOUR OF WOOD BASED MATERIALS USING ACOUSTIC EMISSION ANALYSIS AND IMAGE PROCESSING

Peter Niemz
Institute for Building Materials, Wood Physics, ETH Zürich, Switzerland

Andreas J. Brunner
Empa, Swiss Federal Laboratories for Materials Testing and Research, Dübendorf, Switzerland

Olivier Walter
Institute for Building Materials, Wood Physics, ETH Zürich, Switzerland

ABSTRACT

Tensile strength, modulus of elasticity under tension and failure behaviour were ascertained for particleboards, OSB, plywood and MDF with two raw density grades by means of acoustic emission analysis. The strain distribution over the sample surface under load was determined with video image correlation.

Fracture sites can be predicted relatively well using optical measurements of the deformation under load. A combined observation of narrow and broad surface sides of the specimens is advantageous. Prediction of the cracks is easier for inhomogeneous materials like OSB and plywood than for the more homogeneous materials MDF and particle boards. With the acoustic emission analysis the location of cracks can also be determined to a comparable degree.

KEY WORDS: wood based materials, fracture, Video Image Correlation, acoustic emission, mechanism of failure

INTRODUCTION

Very few investigations exist on the fracture behaviour of wood based materials. Niemz and Hänsel (1987) examined cracking processes by means of acoustic emission, photogrammetry and scanning electron microscopy. A location of the acoustic signals was not possible with the methods then available. Within the scope of this work, the failure behaviour of different wood based materials was examined with the nowadays-improved methods of acoustic emission

analysis (acoustic emission source location) and the ascertainment of displacements via image correlation. The main goal was to analyse the possibilities in order to predict the location of the crack sites. This should generate inputs for the structural optimisation of the materials.

A recapitulatory overview on the fracture behaviour of particle boards was published by Niemz and Hänsel (1987a, 1987b) Hänsel and Niemz (1989) using scanning electron microscopy, photogrammetry and acoustic emission analysis with a single-channel device. A good overview on acoustic emission analysis of wood-based materials is given by Pellerin and Ross (2002). More recent investigations were conducted by, e.g. Aicher et al. (2001), Brunner et al. (2006), Chen et al. (2006) and Kowalski et al. (2004) Other publications about acoustic emission, Video Image Correlation and other methods were publised from Ando et al. (2006), Hänsel (1987), Navi and Guidom (2007), Niemz and Kucera (1999), Vun and Beall (2004).

The particle boards under load initially exhibit elastic deformation of the structural elements and the adhesive joints and subsequently local plastic deformation and micro-cracks as well as displacement between particles. The macroscopic fracture occurs after the formation of local weak points. The sum of the emitted acoustic signals rises exponentially with increasing load. The change of position of individual particles first occurs at local weak points that can be detected with photogrammetry.

The development and improvement of testing methods in recent years allows the detection of such processes on-line and with much higher resolution. Up-to-date video equipment with forthcoming optics permits detection of very small displacements (deflections) on-line and the quantification of them via cross-correlation. Furthermore, multichannel acoustic emission equipment available nowadays provides significantly improved possibilities for signal processing and analysis.

MATERIAL AND METHODS

Material:

The following industrially produced wood based materials were tested:

- MDF
  raw densities: 530 kg.m^{-3} and 760 kg.m^{-3}
  thickness: 16 mm
- OSB
  raw density: 650 kg.m^{-3}
  thickness: 15 mm
  Tests were carried out parallel and perpendicular to the orientation of the strands in the surface layer
- Plywood (Okoumé; 7 layers)
  raw density: 470 kg.m^{-3}
  thickness: 18 mm
- Particleboard
  raw density: 680 kg.m^{-3}
  thickness: 16 mm
- A total of 30 samples per material variant were tested, including 7 samples for the simultaneous acoustic emission analyses and strain determination by means of Video Image Correlation (VIC 2D)

Methodology:

The tests were conducted on tension rods in accordance with DIN 52377 (Fig. 1). Before the actual test, the specimens were conditioned under standard climatic conditions (20°C/65%RH).

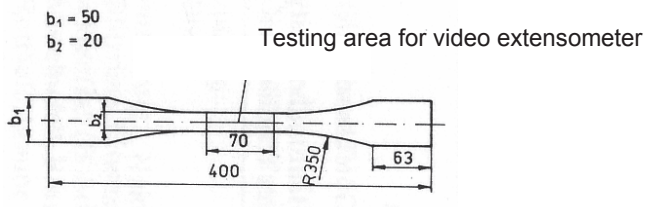

Fig. 1: Dimensions of a tensile specimen according to DIN

Determined properties:

Standard tests

- Raw density according to DIN 52 182
- Moisture content according to DIN 52 183
- Modulus of elasticity under tension and tensile strength parallel to the board plane according to DIN 52 377
-

Testing of the fracture behaviour

- Strain determination by means of Video Image Correlation (VIC 2D)

For the evaluation of the sample deformation under mechanical load, a speckle pattern was applied to the surface of the sample with an airbrush-pistol. Afterwards the displacement of the image points was calculated via cross-correlation.

The following equipment was used:

- for imaging a high resolution video-camera system with distortion free optics and special illumination, and
- the software VIC 2D (Fa. Limess / Germany) for quantitative image evaluation.

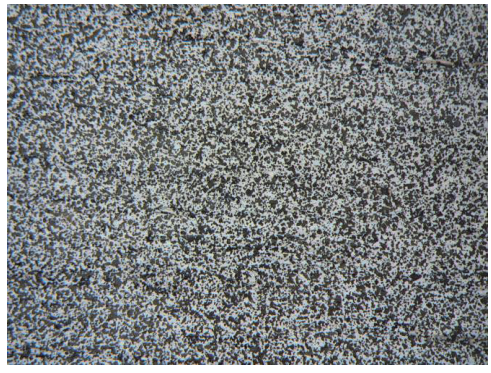

Fig. 2: Speckle pattern under the stereo microscope (20-times magnified)

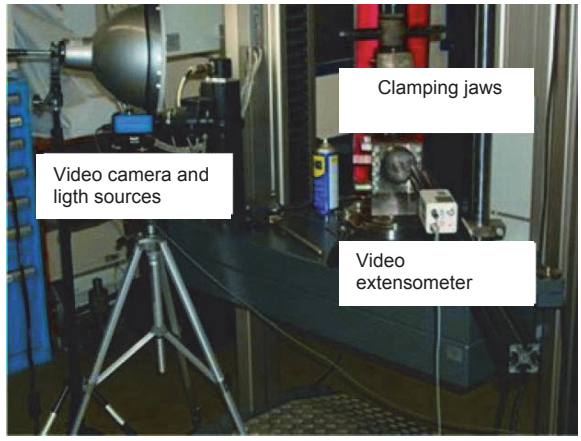

Fig. 3: Experimental setup for the deformation measurement with VIC 2D

Acoustic emission analysis

For the acoustic emission measurements an AMS-3 equipment (*Vallen* / Germany) with 4 SE45-H sensors (Dunegan Engineering Corp.) was used. The sensors are mass-loaded and behave as displacement sensors below 45 kHz (high pass filtering of 30 kHz) and as velocity sensors above 70 kHz (low-pass filtering of 1'000 kHz). Four sensors were necessary for the acoustic location, 2 on each side (Fig. 4). The goal was to combine the signals of the acoustic emission analysis and of the on optical displacement measurement.

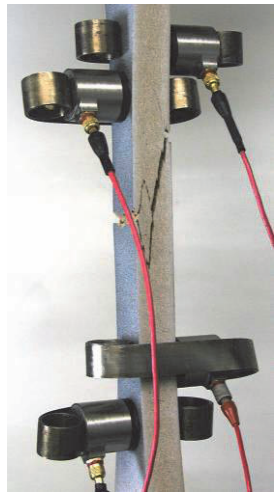

Fig. 4: Position of the 4 sensors for the acoustic emission analysis

Tested parameters:

- Crack location: With the known wave (signal) velocity and signal detection with at least two sensors the origin of an acoustic event can be located (linear location along the plane of the tensile specimen). This was only possible within the panel plane and not in the through-thickness direction because the velocity in the perpendicular direction is only one third of the velocity parallel to the panel plane. The setup shown in Fig. 4 hence allowed only a simplified linear location between the two sensors on either panel plane.
- Number of signals
- Amplitude and signal energy

Fracture characteristics

The fracture characteristics of typical specimens were assessed with a stereomicroscope.

RESULTS AND DISCUSSION

Mechanical properties

Tab. 1 shows a summary of the mechanical properties. A conspicuous difference of the material parameters can be observed regarding the tensile modulus of elasticity, tensile strength as well as fracture strain. MDF showed a higher breaking strain than OSB and plywood. Although showing similar raw density values, the modulus of elasticity of OSB is considerably higher than that for particle boards. There is a slight dependence of the mechanical properties on the orientation of the OSB specimens, namely specimens cut normal to the strand orientation yield slightly lower tensile modulus and strength.

Tab. 1: Material variables (n=30)

Material	Raw density [kg.m^{-3}]	Wood moisture [%]	Tensile modulus of elasticity [N.mm^{-2}]	Tensile strength [N.mm^{-2}]	Fracture strain [%]
MDF 500	530	8.0	1710	10.9	1.34
MDF 700	762	7.5	3141	19.5	1.12
OSB$_{\parallel}$	645	8.3	3501	9.6	0.53
OSB$_{\perp}$	645	8.3	3151	9.2	0.46
Particle board	679	8.9	2023	6.1	0.45
Plywood	470	8.5	3851	19.6	0.59

Ascertainment of the strain distribution with VIC 2D

Selected test specimens were used to determine the displacement under load on the surface of their narrow and broad side. Obvious differences between the tested materials could be observed. The deformation of MDF is very homogenous while OSB shows perspicuous strain peaks due to the considerably larger particles. These differences can easily be seen in Figs. 5 and 6. In Fig. 6 OSB shows elevated displacement (red) in the upper area of the sample.

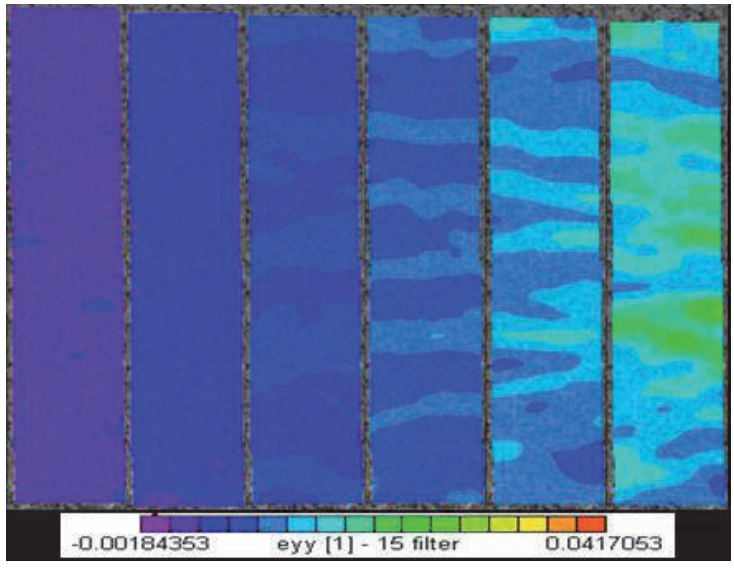

Fig. 5: Strain distribution of MDF 500 with 1%, 20%, 40%, 60%, 80% and 100% (from left to right) of the fracture load

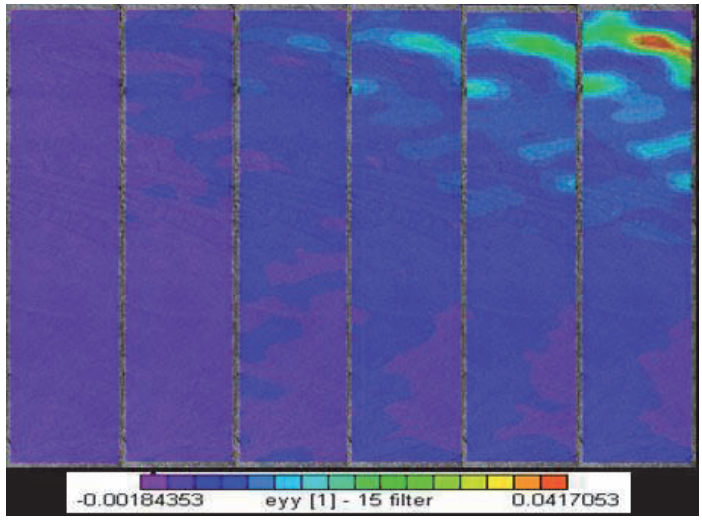

Fig. 6: Strain distribution of OSB_{II} with 1%, 20%, 40%, 60%, 80% and 100% (from left to right) of the fracture load

Fig. 7 shows the strain of plywood under load. The sudden rise of the strain under increasing load can be attributed to the rupture of a central ply lying perpendicular to the load direction.

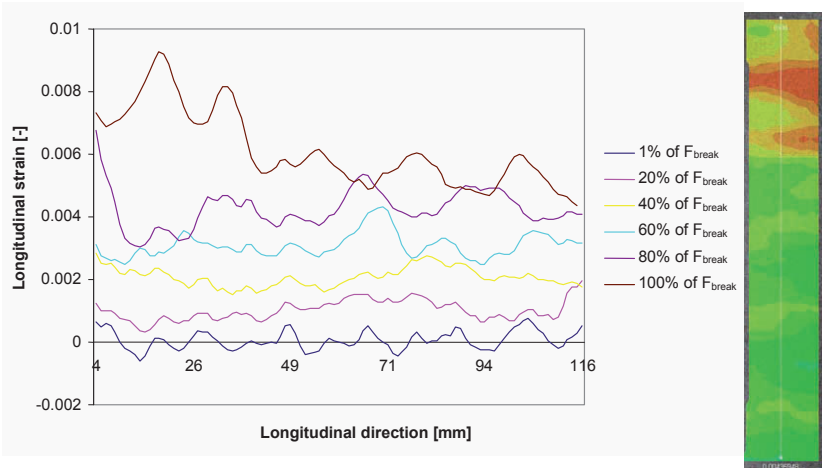

a: strain in longitudinal direction (within panel plane) with 1%, 20%, 40%, 60%, 80% and 100% of the fracture load

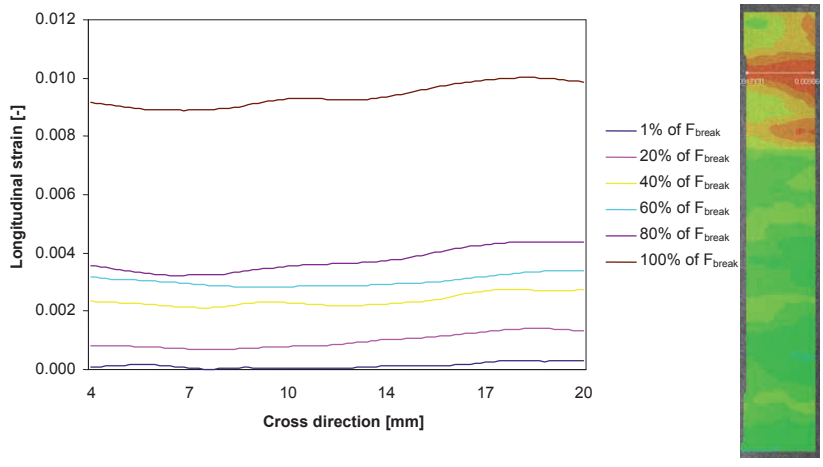

b: strain in transverse direction (perpendicular to the panel plane) with 1%, 20%, 40%, 60%, 80% and 100% of the fracture load

Fig.7: Strain of plywood examining the small surface

Possibilities for the location of the fracture site on the basis of the strain distribution

The strain distribution was used to predict the place of origin of the fracture. Tab. 2 shows the results.

Tab. 2: Comparison of the fracture detection determined with the strain distribution with VIC 2D

Material	Number front view	Number lateral view	Fracture (on broad surface visible [%])	Fracture (on narrow surface visible [%])
MDF 500	12	10	75	43
MDF 700	12	11	64	44
$OSB_{\parallel}$	12	10	63	78
$OSB_{\perp}$	11	10	83	83
Particle board	12	10	40	80
Plywood	13	10	60	78

It is obvious that the fracture site of the MDF is more difficult to predict while observing the narrow surface. On the broad surface the fracture site is easier to discern.

For the other materials the perceptibility of the fracture site was similar for both surfaces. The fracture detection ratio is good for OSB. Here the fracture often occurs between large particles of the surface layer.

Fig. 8 shows the strain along the crack (view on the narrow surface). Already at an early stage weak spots could be distinguished between the particles of the two face layers.

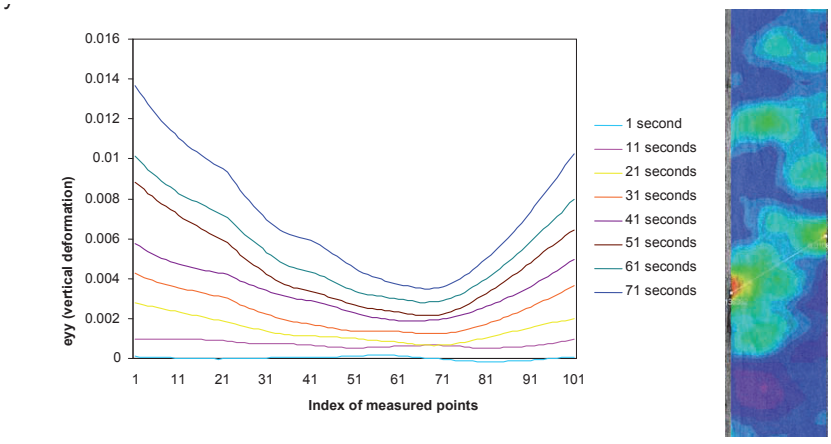

Fig. 8: Longitudinal strain of $OSB_{\parallel}$ along the crack after 1, 11, 21, 31, 41, 51, 61 and 71 seconds

Fig. 9 shows for comparison the failure of MDF 500. The crack initiates at the weakest point of the compound.

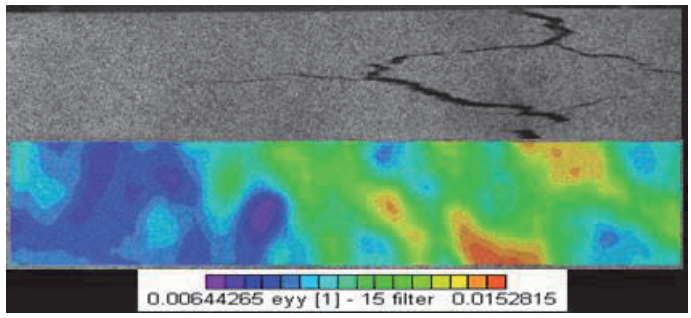

Fig. 9: Fracture site of MDF 500 (red: areas with big strain values in tension direction)

Acoustic emission analysis

Tab. 3 shows important parameters of the acoustic emission analysis for the examined materials, highlighting differences in acoustic emission activity (number of recorded signals during the test) and acoustic emission intensity (signal amplitudes or signal energy).

The largest number of signals was registered for the MDF with the lower raw density. An exponential rise of the cumulative number of signals (or the signal rate, i.e., the number of signals per unit time) was observed under increasing load. The fracture load varied between the materials. Plywood and OSB, the materials with larger structural elements, have higher values for the maximal amplitude and maximal signal energy compared to the MDF panels.

Fig. 10 shows the cumulative acoustic emission energy for the different materials.

For MDF the sensors detect signals yielding a significant rise in cumulative acoustic emission signal energy only at the time of reaching the fracture load, even though acoustic emission signals were recorded right from the start of the test (as for all materials tested). For the other materials, signals yielding a comparable increase in cumulative energy could be detected before the macroscopic failure. The materials show considerable differences concerning their fracture behaviour. Plywood shows the failure of individual layers, while OSB shows fractures perpendicular to the grain within the particles or a change of position of the particles. Fig. 11 shows typical fracture characteristics.

Tab. 3: Acoustic Emission Indicators (Activity and Intensity)

Wood panel type (-)	Average number of AE signals per channel (-)	Maximum AE signal amplitude (dB_{AE})	Maximum AE signal energy (10^8 e.u.)* / number of signals with E > 10^6 e.u. (-)
Medium Density Fiberboard (MDF) 500	4801 ± 888	70 - 75	1.5 – 6.1 / 3 - 8
Medium Density Fiberboard (MDF) 700	3426 ± 642	60 - 70	0.0 – 6.3 / 0 - 4
Oriented Strand Board (OSB) ||	2746 ± 858	90 - 100	0.0 – 30.0 / 3 - 24
Oriented Strand Board (OSB) ⊥	2622 ± 482	85 - 100	0.0 – 16.0 / 1 - 16
Particleboard (PB)	3352 ± 634	85 - 95	0.0 – 8.0 / 0 - 4
Plywood (PW)	3058 ± 349	85 - 100	0.0 – 7.1 / 1 - 26

* e.u. = energy units (time-integral over voltage signal squared)

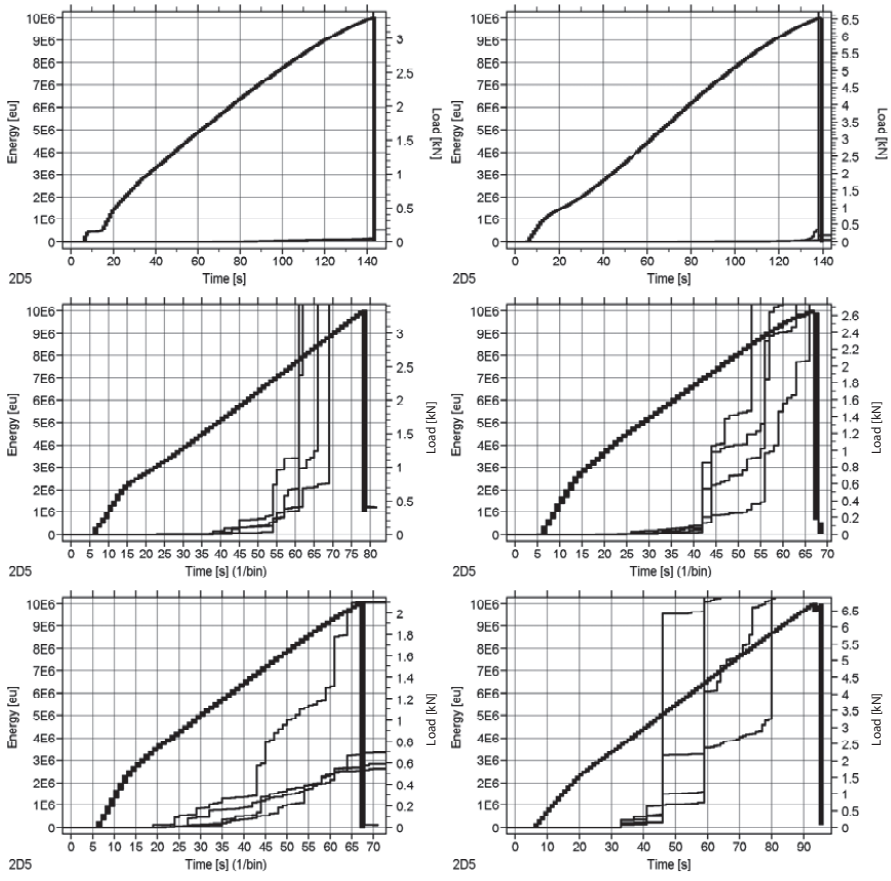

Fig.10: Cumulative acoustic emission signal energy (left hand scale) and load curve (right hand scale) from tensile tests on different types of wood panels, (top left) MDF500, (top right) MDF 700, (middle left) OSB parallel, (middle right) OSB normal, (bottom left) PB, and (bottom right) PW, the thick line indicates the load, the different thin lines the sensors (channels) per specimen

Location of fracture by means of acoustic emission analysis

The location of the signals with an accuracy of 1-2 cm (comparable to sensor diameter) is only possible in the longitudinal direction on the broad surface of the panel plane. The perceptibility, however, significantly varies. The identification of cracks was easier for OSB and plywood due to the bigger size of the structural elements. Local weak spots could be determined as the starting points of the failures. Figs. 12 and 13 show examples for OSB and plywood. In Fig. 13 the displacement ascertained by optical measurements were added. The crack detection is more difficult for MDF because only relatively few signal sources could be located. This is due to the relatively high attenuation in this material, a property that is also reflected by the low signal amplitudes that are recorded. It is hence difficult to identify source clusters indicating crack positions. In plywood the multitude of source locations can also make it difficult to unambiguously identify the cluster indicating the fracture location.

The agreement between observed macroscopic fracture and AE source location clusters is summarized in Tab. 4. MDF and plywood yield the lowest agreement, but for different reasons, as noted above. The agreement for the other types of panels is reasonable and comparable to that obtained from two-dimensional strain measurements. It can be noted that identification of AE source location clusters can be improved by applying additional filtering techniques, at least in the case of plywood, see Brunner (2007). For the analysis presented in Tab. 4, unfiltered AE source location was used and cluster identification was determined by visual assessment of location graphs. The time (or load) at which crack identification becomes possible is also similar for both techniques, roughly at load levels between 50% and 80% of the fracture load.

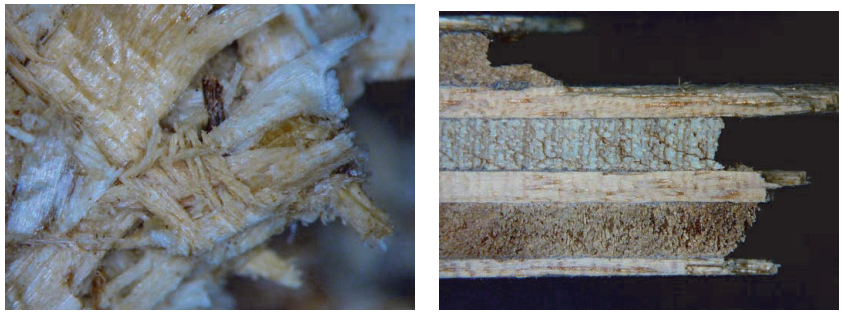

Fig. 11: Fracture characteristics of OSB (left) and plywood (right)

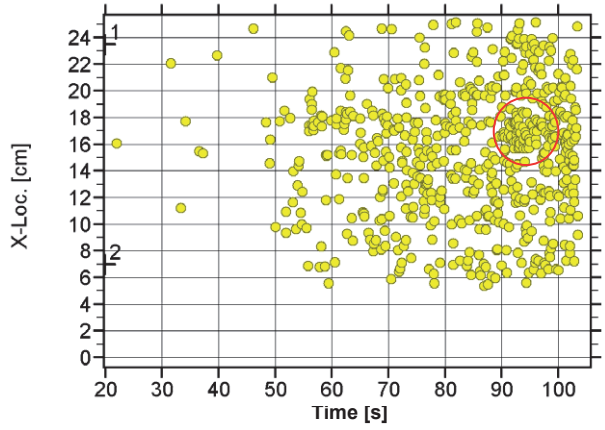

Fig. 12: Located acoustic emission signal sources in a plywood specimen showing cluster formation (red circle) before reaching the fracture load

Fig. 12 shows the crack location on the plywood sample. 1 and 2 correspond to the sensor positions. Between 90 and 100 seconds into the test an accumulation of signals, as well as a cluster between 16 and 18 cm from the lower clamp (red), can be identified. This is the point were the macroscopically visible fracture occurred. One of the central layers that was loaded perpendicular to the grain probably failed simultaneously.

Tab. 4: Acoustic emission source location and agreement with observed macroscopic fracture

Material	Number of specimens with identified AE source location clusters	Total Number of specimens with AE	Number of AE source location clusters within 1 cm from fracture	Percentage of fracture agreeing with AE location
MDF 500	4	6	3	50 %
MDF 700	1	7	1	14 %
$OSB_{\parallel}$	5	5	4	80 %
$OSB_{\perp}$	5	5	4	80 %
Particle board	5	5	4	80 %
Plywood	3	7	1	14 %

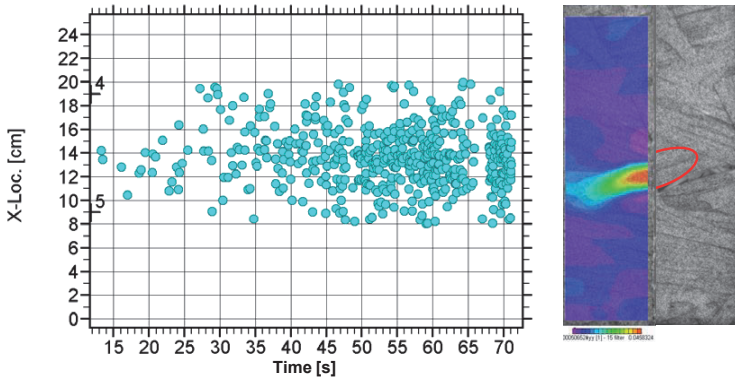

Fig. 13: Crack location of $OSB_{\perp}$ with SEA and VIC2D (longitudinal direction)

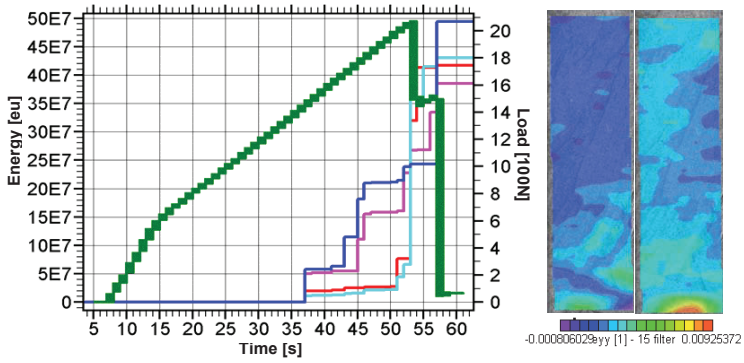

Fig. 14: Cumulative Energy as a function of time and strain distribution of $OSB_{\parallel}$ (broad specimen side). Before and after the energy rise occurring around 53 seconds into the test.

OSB shown in Fig. 13 behaves similarly to plywood. At the time of fracture of the OSB a considerable rise of the energy can be seen (Fig. 14). After the energy rise (53 seconds after the start of the load test) an obvious change of the displacement can be observed.

The two images showing the strain distribution (Fig. 14) were taken one second apart. 53 seconds into the test the rise in cumulative acoustic emission signal energy is clearly visible. Also, in the load-displacement diagram a certain load drop can be observed.

CONCLUSIONS

The mechanical properties of plywood, OSB, particle board and MDF were compared using different methods. Acoustic emission analysis (performed with four sensors) and linear location of acoustic emission signal sources (carried out with two pairs of two sensors, one pair on each broad side of the specimen) and video image correlation were used to determine the displacement of the sample under tensile load. With the measurement of the sample displacement under load it is possible to predict macroscopic fracture sites quite accurately. At these points excessive displacements appear. Displacement measurements are well suited for cracks visible on the sample surface. A combined examination of the narrow and broad side of the specimens would be advantageous, but was not performed since only one strain measurement apparatus was available. The prediction of macroscopic fracture sites is easier for the more inhomogeneous materials, i.e., OSB and particle plywood, than for the homogeneous MDF and particle board. By means of acoustic emission analysis, location of the fracture site is possible within the panel plane to a certain degree. Limitations are the accuracy of the location (affected by anisotropic and inhomogeneous material properties and the correspondingly large differences in wave velocity in particular parallel and perpendicular to the specimen plane) and the identification of acoustic emission source clusters. The latter is affected by signal attenuation in the material on one hand (e.g. for MDF), and by the large number of located signals on the other (e.g. for plywood). The applied method has still considerable potential for further development.

REFERENCES

1. Aicher, S., Höfflin, L., Dill-Langer, G., 2001: Damage evolution and acoustic emission of Wood at tension perpendicular to fiber. Springer-Verlag, Holz als Roh- und Werkstoff 59(1): 104-116
2. Ando, K., Hirashima, Y., Sugihara, M., Hirao, S., Sasaki, Y., 2006: Microscopic processes of shearing fracture of old wood, examined using the acoustic emission technique. J. Wood. Sci. 52(6): 483-489
3. Bodig, J., Jayne, B., 1992: Mechanics of wood and wood composites. Van Norstrand Reinhold, New York, 712 pp.
4. Brunner, A.J., Howald, M., Niemz, P., 2006: Acoustic emission rate behavior of laminated wood specimens under tensile loading. J. Acoust. Emiss. 24(1): 104-110
5. Brunner, A.J., Niemz, P., Walter, O., 2007: Damage accumulation and failure of different types of wood-panels under tensile loading. Proceedings of the American Society for Composites-Twenty-second Technical Conference, Symposium on Wood Composites, No. 13, 16 pp.
6. Chen, Z., Gabbitas, B., Hunt, D., 2006: Monitoring the fracture of wood in torsion using acoustic emission J. Mats. Sci. 41(12): 3645-3655

7. Hänsel, A., 1987: Grundlegende Untersuchungen zur Optimierung der Struktur von Spanplatten“, Ph.D. Thesis, Technical University Dresden (Germany), 212 pp.
8. Kowalski, S.J., Moliński, W., Musielak, G., 2004: The identification of fracture in dried wood based on theoretical modelling and acoustic emission”, Wood Sci. Technol. 38(1): 35-52
9. Navi, P., Guidom, A., 2007: Proceedings of Third International Symposium on Wood Machining. 21-23-5-2007, Lausanne
10. Niemz, P., Hänsel, A., 1987: Untersuchungen zum Verformungs- und Bruchverhalten von Spanplatten. Holztechnologie, (28)3: 139 - 142
11. Hänsel, A., Niemz, P., 1989: Untersuchungen zur Mikromechanik von biegebelasteten Spanplatten. Holzforschung und Holzverwertung 41(3): 47-50
12. Niemz, P., Hänsel, A., 1987: Zur Anwendung der Schallemissionsanalyse in der Holzwerkstoffforschung. Holztechnologie, Leipzig 28(6): 293 - 297
13. Niemz, P., Kucera, L.J., 1999: Untersuchungen zum Einfluss des Faserwinkels auf die Ausbreitungsgeschwindigkeit von Schallwellen in Holz. Holz als Roh und Werkstoff, Berlin (57): 225
14. Pellerin, R., Ross, R.J., 2002: Nondestructive Evaluation of Wood Forest Prod. Society, Madison, 210 pp.
15. Vun, R.Y., Beall, F., 2004: Monitoring creep rupture in oriented strandboard using acoustic emission: Effects of moisture. Holzforschung 58(4): 387-399

Peter Niemz
Institute for Building Materials
Wood Physics
ETH Zürich
Schafmattstrasse 6
CH-8093 Zürich
Switzerland
E-mail: niemzp@ethz.ch

Olivier Walter
Institute for Building Materials
Wood Physics
ETH Zürich
Schafmattstrasse 6
CH-8093 Zürich
Switzerland

Andreas J. Brunner
Empa
Swiss Federal Laboratories for Materials Testing and Research
Überlandstrasse 129
CH- 8600 Dübendorf
Switzerland